Metal–Metal Multiply Bonded Complexes of Technetium. 1. Synthesis and Structural Characterization of Phosphine Complexes That Contain a Tc–Tc Multiple Bond

Carol J. Burns,[1a] Anthony K. Burrell,[1a] F. Albert Cotton,*[,1b] Steven C. Haefner,[1a,b] and Alfred P. Sattelberger*[,1a]

Inorganic and Structural Chemistry Group (CST-3), Chemical Science and Technology Division, Los Alamos National Laboratory, Los Alamos, New Mexico 87545, and Laboratory for Molecular Structure and Bonding, Department of Chemistry, Texas A&M University, College Station, Texas 77843

Received December 3, 1993®

A series of triply metal–metal bonded ditechnetium(II) phosphine complexes with the general formula $Tc_2Cl_4(PR_3)_4$ (PR_3 = PEt_3, PPr^n_3, $PMePh_2$, PMe_2Ph) have been prepared from mononuclear Tc(IV) precursors and fully characterized. Two-electron reduction of the Tc(IV) bis(phosphine) complexes $TcCl_4(PR_3)_2$ (PR_3 = PEt_3, PPr^n_3, $PMePh_2$, PMe_2Ph) with finely divided zinc in aromatic solvents or tetrahydrofuran results in the formation of the corresponding electron-rich triply bonded compounds $Tc_2Cl_4(PR_3)_4$ in high yield. These are the first phosphine complexes of technetium that possess a metal–metal bond. The solid-state structures of the PEt_3, PMe_2Ph, and $PMePh_2$ derivatives have been investigated by X-ray crystallography and are described in detail. The crystallographic parameters for these compounds are as follows: $Tc_2Cl_4(PEt_3)_4$ (**1**), $I\bar{4}3m$ with a = 12.3261(9) Å, V = 1872.7(2) Å^3, and Z = 2; $Tc_2Cl_4(PMe_2Ph)_4$ (**3**), $C2/c$ with a = 17.613(5) Å, b = 9.957(5) Å, c = 23.861(6) Å, β = 117.19(2)°, V = 3722 (2) Å^3, and Z = 4; $Tc_2Cl_4(PMePh_2)_4 \cdot C_6H_6$ (**4**·C_6H_6), $P2_1/c$ with a = 22.910(2) Å, b = 12.286(2) Å, c = 21.550(2) Å, β = 115.867(6)°, V = 5458(1) Å^3, and Z = 4. Similar to the analogous dirhenium(II) complexes, the molecules adopt an eclipsed M_2L_8 conformation with approximate D_{2d} symmetry. The Tc–Tc bond lengths are 2.133(3), 2.127(1), and 2.1384(5) Å for $Tc_2Cl_4(PEt_3)_4$, $Tc_2Cl_4(PMe_2Ph)_4$, and $Tc_2Cl_4(PMePh_2)_4$, respectively. Structural and spectroscopic evidence indicates that these dimers contain an electron-rich Tc–Tc triple bond with a $\sigma^2\pi^4\delta^2\delta^{*2}$ ground-state electronic configuration. Electrochemical studies reveal that each compound undergoes two reversible one-electron oxidation processes, which presumably produce the corresponding Tc_2^{5+} and Tc_2^{6+} dinuclear species. ^{1}H NMR, ^{31}P{^{1}H} NMR, and UV–vis spectroscopic data are presented for each compound.

Introduction

The field of metal–metal multiple-bond chemistry has expanded rapidly in recent years.[2] From its inception, advances made in dirhenium chemistry have contributed significantly to the evolution of this important area of inorganic chemistry. Dirhenium chemistry produced the first examples of complexes containing quadruple and triple metal–metal bonds, and these molecules played a key role in developing an understanding of the physical and chemical properties of multiple bonds between metal atoms. In spite of the rich and diverse chemistry exhibited by dirhenium complexes, the chemistry of metal–metal multiply bonded technetium compounds has remained relatively unexplored. This situation is unusual considering that in groups 6, 8 and 9 nearly all of the major advances in metal–metal bond chemistry have occurred in studies of the second-row congener. However, the development of ditechnetium chemistry has been hindered by the fact that all isotopes of the element are radioactive and the limited availability of technetium-99, a long-lived fission product of uranium-235. Documented examples of metal–metal multiply bonded technetium complexes are relatively rare and include halide dimers and clusters[3] and mixed halide–carboxylate dinuclear species.[4] One example of a tetrakis(hydroxypyridinato) complex has also appeared.[5]

We have now initiated a comprehensive study aimed at further development of the chemistry of metal–metal multiply bonded technetium complexes. The work reported here represents the first in a series of papers describing our recent progress in this area. Such an investigation is particularly timely given the reported applications of low-valent technetium-99m complexes as radiopharmaceuticals.[6] Low-valent mononuclear technetium phosphine compounds, for example, are effective myocardial imaging agents in animals. Studies in the latter area have been aimed at preparing neutral or cationic low-valent technetium species and fine-tuning the physiological properties by careful modification of the ligand environment.[7] While these investigations have focused on the use of mononuclear species, it is conceivable that dinuclear phosphine complexes may be useful either directly as radiopharmaceuticals or as precursors to other low-valent technetium compounds.

In spite of the wealth of chemistry, both redox and nonredox, associated with dinuclear rhenium phosphine complexes of the type $Re_2Cl_4(PR_3)_4$, there has not yet been a single example of an

® Abstract published in *Advance ACS Abstracts,* April 1, 1994.

(1) (a) Los Alamos National Laboratory. (b) Texas A&M University.

(2) Cotton, F. A.; Walton, R. A. *Multiple Bonds Between Metal Atoms*, 2nd ed.; Oxford University Press: New York, 1993.

(3) (a) Eakins, J. D.; Humphreys, D. G.; Mellish, C. E. *J. Chem. Soc.* **1963**, 6012. (b) Bratton, W. K.; Cotton, F. A. *Inorg. Chem.* **1970**, *9*, 789. (c) Preetz, W.; Peters, G. *Z. Naturforsch.* **1980**, *35B*, 797. (d) Cotton, F. A.; Daniels, L. M.; Davison, A.; Orvig, C. *Inorg. Chem.* **1981**, *20*, 3051. (e) Spitsyn, V. I.; Kuzina, A. F.; Oblova, A. A.; Kryuchkov, S. V. *Russ. Chem. Rev. (Engl. Transl.)* **1985**, *54*, 373 and references therein. (f) Peters, G.; Skowronek, J.; Preetz, W. *Z. Naturforsch.* **1992**, *47A*, 591.

(4) (a) Skowronek, J.; Preetz, W.; Jessen, S. M. *Z. Naturforsch.* **1991**, *46B*, 1305. (b) Skowronek, J.; Preetz, W. *Z. Naturforsch.* **1992**, *47B*, 482. (c) Skowronek, J.; Preetz, W. *Z. Anorg. Allg. Chem.* **1992**, *615*, 73. (d) Cotton, F. A.; Gage, L. D. *Nouv. J. Chim.* **1977**, *1*, 441. (e) Koz'min, P. A.; Larina, T. B.; Surazhskaya, M. D. *Koord. Khim.* **1982**, *8*, 851. (f) Koz'min, P. A.; Larina, T. B.; Surazhskaya, M. D. *Koord. Khim.* **1981**, *7*, 1719.

(5) Cotton, F. A.; Fanwick, P. E.; Gage, L. D. *J. Am. Chem. Soc.* **1980**, *102*, 1570.

(6) (a) Deutsch, E.; Vanderheyden, J. L.; Gerundini, P.; Libson, K.; Hirth, W.; Columbo, F.; Savi, A.; Fazio, F. *J. Nucl. Med.* **1987**, *28*, 1870 and references therein. (b) Deutsch, E.; Libson, K.; Vanderheyden, J. L. In *Technetium in Chemistry and Nuclear Medicine*; Nicolini, M., Bandoli, G., Mazzi, U., Eds.; Raven: New York, 1986; Vol. 2, p 161. (c) Jones, A. G.; Abrams, M. J.; Davison, A.; Broadack, J. W.; Toothaker, A. K.; Adelstein, S. J.; Kassis, A. I. *Int. J. Nucl. Med. Biol.* **1984**, *11*, 225. (d) Clarke, M. J.; Pobielski, L. *Coord. Chem. Rev.* **1987**, *78*, 253. (e) Deutsch, E.; Libson, E.; Jurisson, S.; Lindoy, L. F. *Prog. Inorg. Chem.* **1983**, *30*, 75. (f) Deutsch, E.; Libson, K. *Comments Inorg. Chem.* **1984**, *3*, 83. (g) Deutsch, E.; Gerundini, P.; Fazio, F. In *New Procedures in Nuclear Medicine*; Spencer, R. P., Ed.; CRC: Boca Raton, FL; in press. (h) Neves, M.; Libson, K.; Deutsch, E. *Nucl. Med. Biol.* **1987**, *14*, 503.

0020-1669/94/1333-2257$04.50/0

analogous technetium species. In fact, with one exception, all known phosphine complexes of technetium are mononuclear.[8] We now report the rational, high-yield synthesis of several dinuclear technetium phosphine complexes with the general formula $Tc_2Cl_4(PR_3)_4$ from mononuclear precursors. The compounds $Tc_2Cl_4(PR_3)_4$ (PR_3 = PEt_3, PPr^n_3, PMe_2Ph, $PMePh_2$) not only are the first examples of dinuclear technetium phosphine complexes that possess metal–metal bonds but also dramatically expand the number of well-characterized compounds of technetium containing metal–metal triple bonds. The only previous example was found in the extended polymeric chain structure of $[Tc_2Cl_6]_n^{2n-}$.[9] A detailed discussion of the structural and spectroscopic properties of these new M–M bonded compounds of technetium will be presented later in this report.

Experimental Section

General Considerations. *Caution!* The isotope ^{99}Tc is a low-energy β-emitter (E_{max} = 0.292 MeV) with a half-life of 2.12×10^5 years. All manipulations were carried out in laboratories approved for low-level radioactive materials by following procedures and techniques described elsewhere.[10] Ammonium pertechnetate was obtained from Oak Ridge National Laboratory and was purified as described previously.[7f] $TcCl_4(PPh_3)_2$ was prepared from $[NH_4][TcO_4]$ by following a literature procedure.[11] The phosphines, PPh_3 (Strem), $PMePh_2$ (Strem), PMe_2Ph (Strem), PEt_3 (Aldrich), and PPr^n_3 (Strem), were purchased from commercial sources and used without further purification. Toluene, hexanes, heptane, THF, diethyl ether, and hexamethyldisiloxane were distilled under N_2 from either sodium or sodium/potassium alloy. Methylene chloride was distilled from phosphorus pentoxide.

Synthetic Procedures. Unless noted otherwise, the transfer of air-sensitive solids and the workup of air-sensitive reaction mixtures were carried out within the confines of a Vacuum Atmospheres Co. glovebox equipped with a high-capacity purification system (MO-40-2H) and a Dri-Cold freezer maintained at −40 °C. Sonication reactions were performed in sealed Schlenk vessels placed in an ultrasonic cleaning bath (Cole-Parmer 8890).

Preparation of $TcCl_4(PR_3)_2$ (PR_3 = PEt_3, PPr^n_3). In a typical experiment, 2 equiv of phosphine (0.54 mmol) were added to a stirred solution of $TcCl_4(PPh_3)_2$ (0.200 g, 0.26 mmol) in THF (15 mL). The mixture was stirred for approximately 10 min, after which the solvent was removed *in vacuo* to yield a blue residue. The residue was then extracted into benzene (15 mL), and the solution was chromatographed on a silica column. Evaporation of the benzene solution gave $TcCl_4(PR_3)_2$ as a blue solid. Yields: $TcCl_4(PEt_3)_2$, 0.109 g (87%); $TcCl_4(PPr^n_3)_2$, 0.127 g (86%). $TcCl_4(PEt_3)_2$ was characterized by comparison to an authentic sample.[12] The purity of $TcCl_4(PPr^n_3)_2$ was verified by elemental analysis. Anal. Calcd for $C_{18}H_{42}Cl_4P_2Tc$: C, 38.59; H, 7.56. Found: C, 38.94; H, 7.03.

Preparation of $TcCl_4(PR_3)_2$ (PR_3 = PMe_2Ph, $PMePh_2$). In a typical reaction, a quantity of $[NH_4][TcO_4]$ (0.100 g, 0.55 mmol) was suspended in THF (15 mL) and the suspension was treated with chlorotrimethylsilane (0.477 g, 4.4 mmol), rapidly followed by the addition of 5 equiv of phosphine (2.7 mmol). The solution immediately became green after the addition of the phosphine. The mixture was stirred for approximately 10 min, after which the solvent was removed *in vacuo*. The resulting green residue was then extracted with benzene (15 mL), and the extract was chromatographed on a silica gel column. Evaporation of the benzene gave the product as a green solid. Yields: $TcCl_4(PMe_2Ph)_2$, 0.240 g (86%); $TcCl_4(PMePh_2)_2$, 0.211 g (74%). Both compounds were characterized by comparison to authentic samples.[13,14]

Preparation of $Tc_2Cl_4(PEt_3)_4$ (1). Method 1. An amount of $TcCl_4(PEt_3)_2$ (0.100 g, 0.2 mmol) was dissolved in benzene (20 mL), and finely divided Zn (0.136 g, 0.2 mmol) was added. This mixture was placed in a Schlenk tube that was then suspended in an ultrasonic cleaning bath. After 6 h of sonication, the solution color changed from dark green to brown-purple. The mixture was filtered, and the product was precipitated as a pale purple solid by the addition of hexamethyldisiloxane. Yield: 0.082 g (96%). ^1H NMR (C_6D_6, 295 K): δ 2.25 (m, CH_2, 24 H), 1.02 (m, CH_3, 36 H). $^{31}P\{^1H\}$ NMR (C_6D_6, 295 K): δ 47.5. Anal. Calcd for $C_{24}H_{60}Cl_4P_4Tc_2$: C, 35.57; H, 7.46. Found: C, 35.30; H, 7.59.

Method 2. A mixture of $TcCl_4(PEt_3)_2$ (0.500 g, 1.0 mmol) and Zn powder (0.069 g, 1.0 mmol) was heated (50–55 °C) in 10 mL of toluene for 2 days. During this period, the solution color changed from blue-green to brown-purple. The solution was filtered, and the solvent was removed under vacuum. The resulting residue was dissolved in THF (5 mL), and heptane was carefully added to yield a pale purple crystalline solid. The solid was filtered off and washed with heptane. Yield: 0.382 g (90%).

Preparation of $Tc_2Cl_4(PPr^n_3)_4$ (2). $Tc_2Cl_4(PPr^n_3)_4$ was prepared by following the general procedure used in method 1 for the preparation of $Tc_2Cl_4(PEt_3)_4$. Yield: 0.081 g (93%). ^1H NMR (C_6D_6, 295 K): δ 2.33 (m, CH_2, 24 H), 1.51 (m, CH_2, 24 H), 0.99 (m, CH_3, 36 H). ^{31}P NMR (C_6D_6, 295 K): δ 44.3. Anal. Calcd for $C_{36}H_{84}Cl_4P_4Tc_2$: C, 44.18; H, 8.65. Found: C, 43.88; H, 8.30.

Preparation of $Tc_2Cl_4(PMe_2Ph)_4$ (3). A mixture of $TcCl_4(PMe_2Ph)_2$ (0.100 g, 0.19 mmol) and Zn powder (0.013 g, 0.19 mmol) was suspended in THF (20 mL), and the suspension was sonicated for 6 h. During this period, the solids dissolved and the solution color changed from dark green to purple-red. The solution was filtered, and the solvent was removed *in vacuo*. The resulting residue was extracted into benzene and recrystallized by the careful addition of $(SiMe_3)_2O$. If necessary, the product may be further purified by column chromatography (silica gel/benzene). Yield: 0.083 g (97%). ^1H NMR (C_6D_6, 295 K): δ 7.62 (m, Ar H, 12 H), 6.99 (m, Ar H, 8 H), 1.60 (t, CH_3, 24 H). $^{31}P\{^1H\}$ NMR (C_6D_6, 295 K): δ 42.6. Anal. Calcd for $C_{32}H_{44}Cl_4P_4Tc_2$: C, 43.17; H, 4.98. Found: C, 43.22; H, 5.31.

Preparation of $Tc_2Cl_4(PMePh_2)_4$ (4). $Tc_2Cl_4(PMePh_2)_4$ was prepared from $TcCl_4(PMePh_2)_2$ in a manner similar to that described for $Tc_2Cl_4(PMe_2Ph)_4$. If required, the product may be further purified by chromatography on a silica gel column. Yield: 0.084 g (94%). The compound crystallizes as a benzene solvate which loses benzene upon drying *in vacuo*. ^1H NMR (C_6D_6, 295 K): δ 7.63 (m, Ar H, 24 H), 6.99 (m, Ar H, 16 H), 1.60 (t, CH_3, 12 H). $^{31}P\{^1H\}$ NMR (C_6D_6, 295 K): δ 39.5. Anal. Calcd for $C_{52}H_{52}Cl_4P_4Tc_2$: C, 54.85; H, 4.60. Found: C, 55.08; H, 4.55.

Physical Measurements. ^1H and $^{31}P\{^1H\}$ NMR spectral measurements were obtained on a Bruker WM-300 spectrometer operating at 300 and 121.5 MHz, respectively. ^1H chemical shifts are referenced to the residual proton impurity in the deuterated solvent. $^{31}P\{^1H\}$ chemical shifts are reported relative to an external standard of 85% H_3PO_4. Electronic absorption spectra were measured on a Hewlett-Packard 8450A spectrophotometer. Electrochemical measurements were performed on an EG&G Princeton Applied Research Model 273 potentiostat. Cyclic voltammetry experiments were carried out at room temperature in CH_2Cl_2 using 0.2 M $[^nBu_4N][BF_4]$ as a supporting electrolyte. A platinum disk working electrode and a platinum wire counter electrode were used in conjunction with a silver wire quasi-reference electrode which was separated from the bulk solution by a fine-porosity glass frit for electrochemical measurements. $E_{1/2}$ values, determined as $(E_{p,a} + E_{p,c})/2$, are reported relative to an internal ferrocene standard. Elemental analyses were obtained on a Perkin-Elmer 2400 analyzer.

X-ray Crystallographic Procedures. Crystallographic data for $Tc_2Cl_4(PEt_3)_4$ (**1**), $Tc_2Cl_4(PMe_2Ph)_4$ (**3**), and $Tc_2Cl_4(PMePh_2)_4 \cdot C_6H_6$

(7) For example, see: (a) Konno, T.; Heeg, M.; Stuckey, J. A.; Kirchhoff, J. R.; Heineman, W. R.; Deutsch, E. *Inorg. Chem.* **1992**, *31*, 1173. (b) Konno, T.; Seeber, R.; Kirchhoff, J. R.; Heineman, W. R.; Deutsch, E.; Heeg, M. J. *Transition Met. Chem. (London)* **1993**, *18*, 209. (c) Konno, T.; Heeg, M. J.; Deutsch, E. *Inorg. Chem.* **1989**, *28*, 1694. (d) Konno, T.; Kirchhoff, J. R.; Heineman, W. R.; Deutsch, E. *Inorg. Chem.* **1989**, *28*, 1174. (e) Konno, T.; Heeg, M. J.; Deutsch, E. *Inorg. Chem.* **1988**, *27*, 4113. (f) Libson, K.; Barnett, B. L.; Deutsch, E. *Inorg. Chem.* **1983**, *22*, 1695. (g) Libson, K.; Doyle, M. N.; Thomas, R. W.; Nelesnik, T.; Woods, M.; Sullivan, J. C.; Elder, R. C.; Deutsch, E. *Inorg. Chem.* **1988**, *27*, 3614. (h) Bandoli, G.; Mazzi, U.; Ichimura, A.; Libson, K.; Heineman, W. R.; Deutsch, E. *Inorg. Chem.* **1984**, *23*, 2898. (i) Vanderheyden, J.-L.; Ketring, A. R.; Libson, K.; Heeg, M. J.; Roecker, L.; Motz, P.; Whittle, R.; Elder, R. C.; Deutsch, E. *Inorg. Chem.* **1984**, *23*, 2184. (j) Hurst, R. W.; Heineman, W. R.; Deutsch, E. *Inorg. Chem.* **1981**, *20*, 3298. (k) Ichimura, A.; Heineman, W. R.; Vanderheyden, J.-L.; Deutsch, E. *Inorg. Chem.* **1984**, *23*, 1272.

(8) Tisato, F.; Refosco, F.; Mazzi, U.; Bandoli, G.; Nicolini, M. *Inorg. Chim. Acta* **1989**, *157*, 227.

(9) (a) Cotton, F. A.; Daniels, L. M.; Falvello, L. R.; Grigoriev, M. S.; Kryuchkov, S. V. *Inorg. Chim. Acta* **1991**, *189*, 53. (b) Kryuchkov, S. V.; Grigoriev, M. S.; Kuzina, A. F.; Gulev, B. F.; Spitsyn, V. I. *Dokl. Akad. Nauk. SSSR* **1986**, 389; *Dokl. Chem.* **1986**, 147.

(10) Bryan, J. C.; Burrell, A. K.; Miller, M. M.; Smith, W. H.; Burns, C. J.; Sattelberger, A. P. *Polyhedron* **1993**, *12*, 1769 and references therein.

(11) Fergusson, J. E.; Heveldt, P. F. *J. Inorg. Nucl. Chem.* **1976**, *38*, 2231.

(12) Rochon, F. D.; Melanson, R.; Kong, P. C. *Acta Crystallogr., Sect. C* **1991**, *C47*, 732.

(13) Mazzi, U.; De Paoli, G.; Traverso, O. *J. Inorg. Nucl. Chem.* **1977**, *39*, 1090.

(14) Cotton, F. A.; Day, C. S.; Diebold, M. P.; Roth, W. J. *Acta Crystallogr., Sect. C* **1990**, *C46*, 1623.

Table 1. Crystallographic Data for $Tc_2Cl_4(PEt_3)_4$ (**1**), $Tc_2Cl_4(PMe_2Ph)_4$ (**3**), and $Tc_2Cl_4(MePh_2)_4 \cdot C_6H_6$ (**4**·C_6H_6)

	1	**3**	**4**·C_6H_6
formula	$C_{24}H_{60}Cl_4P_4Tc_2$	$C_{32}H_{44}Cl_4P_4Tc_2$	$C_{58}H_{58}Cl_4P_4Tc_2$
fw	810.45	890.35	1216.72
space group	$I\bar{4}3m$	$C2/c$	$P2_1/c$
a, Å	12.3261(9)	17.613(5)	22.910(2)
b, Å		9.957(5)	12.286(2)
c, Å		23.861(6)	21.550(2)
α, deg			
β, deg		117.19(2)	115.867(6)
γ, deg			
V, Å^3	1872.7(2)	3722(2)	5458(1)
Z	2	4	4
ρ_{calc}, g/cm^3	1.437	1.589	1.481
μ, cm^{-1}	103.25 (Cu Kα)	12.24 (Mo Kα)	73.09 (Cu Kα)
transm coeff: max–min	1.00–0.88	1.00–0.79	1.00–0.55
radiation (monochromated in incident beam)	Cu Kα	Mo Kα	Cu Kα
λ_α, Å	1.541 84	0.710 73	1.541 84
temp, °C	20 ± 2	20 ± 2	20 ● 2
$R(F_o)^a$ ($F_o^2 > 2\sigma(F_o^2)$)	0.045	0.025	0.035
$R_w(F_o^2)^b$ (all data)	0.111	0.066	0.100
quality-of-fit indicator^c	1.14	1.14	1.08

^{a} $R = \Sigma||F_o| - |F_c||/\Sigma|F_o|$. ^{b} $R_w = [\Sigma[w(F_o^2 - F_c^2)^2]/\Sigma[w(F_o^2)^2]]^{1/2}$. ^{c} Quality of fit = $[\Sigma[w(F_o^2 - F_c^2)^2]/(N_{observns} - N_{params})]^{1/2}$; based on all data.

Table 2. Atomic Coordinates and Equivalent Isotropic Displacement Parameters for $Tc_2Cl_4(PEt_3)_4$ (**1**)

	x	y	z	U_{eq},^{a} Å^2
Tc(1)	0.0865(1)	0	0	0.062(1)
Cl(1)	0.1380(2)	0.1380(2)	–0.1380(2)	0.117(2)
P(1)	0.1360(2)	0.1360(2)	0.1360(2)	0.091(2)
Cl1)	0.115(1)	0.115(1)	0.2765(8)	0.24(1)
C(2)	0.105(3)	0.161(2)	0.356(3)	0.28(2)

^{a} Equivalent isotropic U_{eq} is defined as one-third of the trace of the orthogonalized U_{ij} tensor. The following occupancy factors were used for disordered atoms: Tc(1), 0.33; C(2), 0.5.

Table 3. Atomic Coordinates and Equivalent Isotropic Displacement Parameters for $Tc_2Cl_4(PMe_2Ph)_4$ (**3**).

	x	y	z	U_{eq},^{a} Å^2
Tc(1)	0.4473(1)	0.5204(1)	0.2041(1)	0.028(1)
Tc(1a)	0.5000	0.6206(11)	0.2500	0.038(3)
Tc(1b)	0.5000	0.4094(10)	0.2500	0.037(3)
Cl(1)	0.4695(1)	0.6877(1)	0.1410(1)	0.046(1)
Cl(2)	0.3516(1)	0.3478(1)	0.2023(1)	0.044(1)
P(1)	0.4857(1)	0.3606(1)	0.1428(1)	0.038(1)
P(2)	0.3475(1)	0.6810(1)	0.2108(1)	0.040(1)
C(1)	0.4915(3)	0.1825(5)	0.1615(2)	0.056(1)
C(2)	0.5835(3)	0.3891(6)	0.1370(2)	0.054(1)
C(3)	0.4033(3)	0.3677(5)	0.0604(2)	0.041(1)
C(4)	0.4208(4)	0.3236(6)	0.0125(3)	0.067(2)
C(5)	0.3578(4)	0.3260(7)	–0.0494(2)	0.072(2)
C(6)	0.2786(4)	0.3722(5)	–0.0649(3)	0.062(2)
C(7)	0.2601(4)	0.4151(6)	–0.0179(3)	0.061(2)
C(8)	0.3219(3)	0.4137(5)	0.0443(2)	0.050(1)
C(9)	0.3749(4)	0.8581(5)	0.2198(3)	0.062(2)
C(10)	0.3040(3)	0.6577(6)	0.2657(2)	0.062(2)
C(11)	0.2531(3)	0.6696(5)	0.1339(2)	0.041(1)
C(12)	0.1932(3)	0.5703(6)	0.1226(3)	0.056(1)
C(13)	0.1226(3)	0.5579(6)	0.0631(3)	0.064(2)
C(14)	0.1121(3)	0.6461(6)	0.0161(3)	0.056(1)
C(15)	0.1707(3)	0.7444(6)	0.0268(2)	0.058(2)
C(16)	0.2408(3)	0.7554(5)	0.0853(2)	0.048(1)

^{a} Equivalent isotropic U_{eq} is defined as one-third of the trace of the orthogonalized U_{ij} tensor. The following occupancy factors were used for disordered atoms: Tc(1), 0.943; Tc(1a), 0.028; Tc(1b), 0.028.

(**4**·C_6H_6) were obtained using general procedures that have been fully described elsewhere.[15] All calculations were performed on a local-area VAX cluster at Texas A&M University employing a VAX/VMS V4.6 computer. Data were corrected for Lorentz and polarization effects. Final least-squares refinement for each structure was performed using the SHELXL-93 structure refinement program.[16] Crystallographic parameters and basic information pertaining to data collection and structure refinement are summarized in Table 1. A listing of positional and isotropic parameters for compounds **1**, **3**, and **4**·C_6H_6 will be found in Tables 2–4. Selected bond distances and angles are listed in Tables 5-7 for compounds **1**, **3**, and **4**·C_6H_6. Tables of anisotropic displacement parameters as well as complete tables of bond distances and angles are available as supplementary material.

$Tc_2Cl_4(PEt_3)_4$ (1). Single crystals of $Tc_2Cl_4(PEt_3)_4$ were grown by slow evaporation of a solution of **1** in a mixture of benzene and hexamethyldisiloxane. A block-shaped crystal with approximate dimensions of 0.25 × 0.30 × 0.30 mm^3 was covered with a thin layer of epoxy resin and placed on the tip of a glass fiber. Least-squares refinement of 23 carefully centered reflections in the range $70 < 2\theta < 105°$ resulted in cell parameters consistent with a body-centered cubic lattice. The lattice symmetry was confirmed by axial photographs. Intensity data were collected at ambient temperature on a Rigaku AFC5R diffractometer equipped with a rotating Cu radiation source ($\lambda_{Cu\ K\alpha}$ = 1.54184 Å). In order to determine the absolute configuration, Bijvoet pairs were collected. A total of 881 data in the range $4 \le 2\theta \le 120°$ were measured using a θ–2θ scan technique. Periodic monitoring of three representative reflections revealed no loss in crystal integrity throughout data collection. An absorption correction based on azimuthal scans of several reflections with Eulerian angle χ near 90° was applied to the data. Equivalent data were averaged (R_{merge} = 0.04) except those that corresponded to Bijvoet pairs.

The technetium atom was positioned using the coordinates of the rhenium atom from the isomorphous structure of $Re_2Cl_4(PEt_3)_4$.[17] The remaining chlorine, phosphorus, and carbon atoms were found from a subsequent least-squares refinement and difference Fourier map. Refinement was carried out in the noncentrosymmetric space group $I\bar{4}3m$ which requires no scrambling of the Cl^- and PR_3 ligands. Previous refinement of $Re_2Cl_4(PEt_3)_4$ showed that much worse figures of merit were obtained for refinement in $Im\bar{3}m$ than in $I\bar{4}3m$.[17] The absolute configuration of $Tc_2Cl_4(PEt_3)_4$ was established by the method described by Flack (Flack x parameter = –0.06(9)).[18] Final anisotropic refinement of 26 parameters converged with R (based on F for all data) of 0.058 and R_w (based on F^2 for all data) of 0.111.[19] The goodness-of-fit based on F^2 was 1.14, and the highest peak in the final difference map was 0.22 e/Å^3.

$Tc_2Cl_4(PMe_2Ph)_4$ (3). Acicular crystals of $Tc_2Cl_4(PMe_2Ph)_4$ were obtained by slow evaporation of a solution of **3** in a mixture of benzene and hexamethyldisiloxane. A crystal with the approximate dimensions of 0.05 × 0.40 × 0.60 mm^3 was coated with a thin layer of epoxy cement and placed on the end of a glass fiber. Cell parameters consistent with that of a C-centered monoclinic lattice were obtained by least-squares refinement of 21 well-centered reflections in the range $25 < 2\theta < 34°$. The cell choice was confirmed by axial photography. Data

(15) (a) Bino, A.; Cotton, F. A.; Fanwick, P. E. *Inorg. Chem.* **1979**, *18*, 3558. (b) Cotton, F. A.; Frenz, B. A.; Deganello, G.; Shaver, A. *J. Organomet. Chem.* **1979**, *50*, 227.
(16) Sheldrick, G. M. SHELXL-93. Institut für Anorganische Chemie der Universität Göttingen, Göttingen, Germany, 1993.
(17) Cotton, F. A.; Daniels, L. M.; Shang, M.; Yao, Z. *Inorg. Chim. Acta* **1994**, *215*, 103.
(18) Flack, H. D. *Acta Crystallogr., Sect. A* **1983**, *A37*, 22.
(19) R factors based on F^2 are statistically about twice as large as those based on F.

Table 4. Atomic Coordinates and Equivalent Isotropic Displacement Parameters for $Tc_2Cl_4(PMePh_2)_4 \cdot C_6H_6$ ($4 \cdot C_6H_6$)

	x	y	z	U_{eq},[a] Å^2
Tc(1)	0.2614(1)	0.1312(1)	0.8194(1)	0.035(1)
Tc(2)	0.1734(1)	0.0669(1)	0.7410(1)	0.033(1)
P(1)	0.2827(1)	0.2929(1)	0.7637(1)	0.043(1)
P(2)	0.2833(1)	0.0103(1)	0.9195(1)	0.044(1)
P(3)	0.2139(1)	−0.0590(1)	0.6778(1)	0.040(1)
P(4)	0.0904(1)	0.1643(1)	0.7648(1)	0.037(1)
Cl(1)	0.3536(1)	0.0615(1)	0.8098(1)	0.052(1)
Cl(2)	0.2440(1)	0.2599(1)	0.8910(1)	0.048(1)
Cl(3)	0.1459(1)	−0.0975(1)	0.7803(1)	0.049(1)
Cl(4)	0.1309(1)	0.1777(1)	0.6405(1)	0.046(1)
C(1)	0.2591(3)	0.2660(4)	0.6873(3)	0.061(1)
C(2)	0.3602(1)	0.3550(4)	0.8230(3)	0.051(1)
C(3)	0.3846(3)	0.4409(5)	0.8002(3)	0.073(2)
C(4)	0.4437(3)	0.4886(6)	0.8443(4)	0.089(2)
C(5)	0.4772(3)	0.4506(6)	0.9090(4)	0.089(2)
C(6)	0.4533(3)	0.3673(6)	0.9323(3)	0.084(2)
C(7)	0.3947(3)	0.3189(5)	0.8897(3)	0.065(2)
C(8)	0.2300(2)	0.4120(4)	0.7402(2)	0.046(1)
C(9)	0.2325(3)	0.4836(4)	0.7906(3)	0.056(1)
C(10)	0.1922(3)	0.5736(5)	0.7741(4)	0.075(2)
C(11)	0.1486(3)	0.5920(5)	0.7068(4)	0.084(2)
C(12)	0.1460(3)	0.5237(5)	0.6567(3)	0.080(2)
C(13)	0.1861(3)	0.4328(4)	0.6724(3)	0.066(2)
C(14)	0.2217(2)	0.0130(5)	0.9508(3)	0.058(1)
C(15)	0.3051(2)	−0.1348(4)	0.9252(2)	0.053(1)
C(16)	0.3519(3)	−0.1695(5)	0.9047(3)	0.062(1)
C(17)	0.3704(3)	−0.2768(5)	0.9119(3)	0.076(2)
C(18)	0.3441(3)	−0.3508(5)	0.9402(4)	0.090(2)
C(19)	0.2984(3)	−0.3191(5)	0.9598(4)	0.091(2)
C(20)	0.2784(3)	−0.2107(5)	0.9525(3)	0.073(2)
C(21)	0.3548(2)	0.0694(4)	0.9908(2)	0.050(1)
C(22)	0.3509(3)	0.1225(5)	1.0452(3)	0.067(2)
C(23)	0.4059(3)	0.1669(6)	1.0981(3)	0.087(2)
C(24)	0.4645(3)	0.1633(6)	1.0965(3)	0.084(2)
C(25)	0.4680(3)	0.1148(6)	1.0408(3)	0.086(2)
C(26)	0.4143(3)	0.0689(6)	0.9886(3)	0.076(2)
C(27)	0.2639(2)	−0.1700(4)	0.7286(2)	0.051(1)
C(28)	0.1469(2)	−0.1300(4)	0.6075(2)	0.045(1)
C(29)	0.0845(3)	−0.0912(5)	0.5799(3)	0.062(1)
C(30)	0.0354(3)	−0.1426(5)	0.5247(3)	0.073(2)
C(31)	0.0481(3)	−0.2331(5)	0.4966(3)	0.068(2)
C(32)	0.1104(3)	−0.2717(5)	0.5224(3)	0.075(2)
C(33)	0.1594(3)	−0.2208(4)	0.5774(3)	0.065(1)
C(34)	0.2574(2)	−0.0065(4)	0.6297(2)	0.045(1)
C(35)	0.2220(3)	0.0504(4)	0.5686(2)	0.053(1)
C(36)	0.2523(3)	0.0929(5)	0.5318(3)	0.065(2)
C(37)	0.3175(3)	0.0817(5)	0.5536(3)	0.072(2)
C(38)	0.3530(3)	0.0245(5)	0.6133(3)	0.072(2)
C(39)	0.3231(3)	−0.0199(5)	0.6514(3)	0.058(1)
C(40)	0.0928(2)	0.3115(4)	0.7602(2)	0.047(1)
C(41)	0.0785(2)	0.1375(4)	0.8424(2)	0.041(1)
C(42)	0.0486(2)	0.0425(4)	0.8465(3)	0.053(1)
C(43)	0.0388(3)	0.0184(5)	0.9040(3)	0.070(2)
C(44)	0.0595(3)	0.0912(6)	0.9581(3)	0.075(2)
C(45)	0.0894(3)	0.1858(6)	0.9548(3)	0.072(2)
C(46)	0.0989(2)	0.2101(4)	0.8969(2)	0.053(1)
C(47)	0.0092(2)	0.3683(4)	0.1983(2)	0.041(1)
C(48)	−0.0033(2)	0.4660(4)	0.1626(3)	0.053(1)
C(49)	−0.0651(3)	0.4898(5)	0.1131(3)	0.061(1)
C(50)	−0.1151(3)	0.4171(5)	0.0998(3)	0.067(2)
C(51)	−0.1034(2)	0.3220(5)	0.1352(3)	0.063(1)
C(52)	−0.0421(2)	0.2977(4)	0.1843(3)	0.054(1)
C(53)	0.4821(8)	0.8090(9)	0.2473(5)	0.164(4)
C(54)	0.4252(9)	0.782(1)	0.222(1)	0.271(9)
C(55)	0.3919(6)	0.793(1)	0.160(1)	0.35(1)
C(56)	0.416(1)	0.831(1)	0.1238(7)	0.38(1)
C(57)	0.472(1)	0.857(1)	0.149(1)	0.33(1)
C(58)	0.5068(6)	0.846(1)	0.211(1)	0.34(1)

[a] Equivalent isotropic U_{eq} is defined as one-third of the trace of the orthogonalized U_{ij} tensor.

collection was performed at 20 ± 2 °C on a Syntex P3 diffractometer equipped with graphite monochromated Mo radiation ($\lambda_{Mo\ K\alpha}$ = 0.710 73 Å). A total of 2038 data were collected in the range $4 \le 2\theta \le 50°$ using a θ–2θ scan technique. Three representative reflections were measured a regular intervals and revealed that there was no decay in diffraction intensity. An absorption correction based on azimuthal scans of several reflections with Eulerian angle χ near 90° was applied to the data. After averaging of equivalent reflections, a total of 1929 data remained with $F_o^2 > 2\sigma(F_o^2)$. Examination of the systematic absences led to the selection of $C2/c$ as the space group. This choice was later confirmed by successful least-squares refinement in this space group. The positions of the metal atoms and those of the associated ligands were determined by a Patterson synthesis. After initial refinement of all non-hydrogen atoms, it became apparent that a second orientation of the Tc–Tc unit was present along the crystallographic 2-fold axis that bisected the molecule. The occupancies of the two Tc_2 units were initially set at 0.95 and 0.05. These values were allowed to refine, resulting in final occupancies of 94.3% and

Table 5. Selected Bond Lengths (Å) and Angles (deg) for $Tc_2Cl_4(PEt_3)_4$ (**1**)[a]

Tc(1)–Tc(1)^i	2.133(3)	P(1)–C(1)	1.769(12)
Tc(1)–P(1)	2.448(3)	C(1)–C(2)	1.14(3)
Tc(1)–Cl(1)	2.488(4)		
Tc(1)^i–Tc(1)–P(1)	104.43(5)	P(1)–Tc(1)–P(1)^{iii}	151.15(10)
Tc(1)^i–Tc(1)–Cl(1)	104.78(5)	P(1)–Tc(1)–Cl(1)	86.36(2)
Cl(1)–Tc(1)–Cl(1)^{ii}	150.45(9)	C(1)–P(1)–C(1)^{iv}	105.2(9)
C(1)–P(1)–Tc(1)	122.4(8)	C(1)^{ii}–P(1)–Tc(1)	122.4(8)
C(1)^{iv}–P(1)–Tc(1)	92.7(8)	C(2)–C(1)–P(1)	142(3)

[a] Symmetry transformations used to generate equivalent atoms: (i) $-x, y, -z$; (ii) y, z, x; (iii) $x, -y, -z$; (iv) z, x, y.

Table 6. Selected Bond Lengths (Å) and Angles (deg) for $Tc_2Cl_4(PMe_2Ph)_4$ (**3**)

Tc(1)–Tc(1)*	2.127(1)	Tc(1)–Cl(2)	2.392(1)
Tc(1)–Cl(1)	2.396(1)	Tc(1)–P(2)	2.435(1)
Tc(1)–P(1)	2.457(1)	P(1)–C(2)	1.812(5)
P(1)–C(1)	1.821(5)	P(1)–C(3)	1.835(5)
P(2)–C(10)	1.808(5)	P(2)–C(9)	1.815(6)
P(2)–C(11)	1.833(5)		
Tc(1)*–Tc(1)–Cl(2)	107.18(4)	Tc(1)*–Tc(1)–Cl(1)	109.30(4)
Tc(1)*–Tc(1)–P(1)	105.32(4)	Tc(1)*–Tc(1)–P(2)	104.44(4)
Cl(2)–Tc(1)–Cl(1)	143.50(5)	Cl(1)–Tc(1)–P(2)	85.11(5)
Cl(2)–Tc(1)–P(2)	87.12(5)	Cl(2)–Tc(1)–P(1)	84.70(5)
Cl(1)–Tc(1)–P(1)	84.64(5)	P(2)–Tc(1)–P(1)	150.24(5)
C(2)–P(1)–C(1)	102.9(3)	C(2)–P(1)–C(3)	103.1(2)
C(1)–P(1)–C(3)	103.2(2)	C(2)–P(1)–Tc(1)	118.3(2)
C(1)–P(1)–Tc(1)	119.0(2)	C(3)–P(1)–Tc(1)	108.3(2)
C(10)–P(2)–C(9)	102.6(3)	C(10)–P(2)–C(11)	103.1(2)
C(9)–P(2)–C(11)	104.4(2)	C(10)–P(2)–Tc(1)	121.4(2)
C(9)–P(2)–Tc(1)	119.0(2)	C(11)–P(2)–Tc(1)	104.2(2)
C(8)–C(3)–C(4)	118.0(5)	C(8)–C(3)–P(1)	121.6(4)
C(4)–C(3)–P(1)	120.5(4)	C(16)–C(11)–P(2)	121.8(4)
C(12)–C(11)–P(2)	120.2(4)	C(12)–C(11)–C(16)	118.0(4)

Table 7. Selected Bond Lengths (Å) and Angles (deg) for $Tc_2Cl_4(PMePh_2)_4 \cdot C_6H_6$ ($4 \cdot C_6H_6$)

Tc(1)–Tc(2)	2.1384(5)	Tc(1)–Cl(2)	2.361(1)
Tc(1)–Cl(1)	2.370(1)	Tc(1)–P(1)	2.478(1)
Tc(1)–P(2)	2.483(1)	Tc(2)–Cl(4)	2.377(1)
Tc(2)–Cl(3)	2.377(1)	Tc(2)–P(4)	2.481(1)
Tc(2)–P(3)	2.493(1)	P(1)–C(1)	1.819(5)
P(1)–C(8)	1.823(5)	P(1)–C(2)	1.841(5)
P(2)–C(14)	1.810(5)	P(2)–C(21)	1.838(5)
P(2)–C(15)	1.841(5)	P(3)–C(27)	1.810(5)
P(3)–C(28)	1.839(5)	P(3)–C(34)	1.838(4)
P(4)–C(40)	1.814(5)	P(4)–C(47)	1.831(4)
P(4)–C(41)	1.837(4)		
Tc(2)–Tc(1)–Cl(2)	113.20(3)	Tc(2)–Tc(1)–Cl(1)	111.49(3)
Tc(2)–Tc(1)–P(2)	103.21(3)	Tc(2)–Tc(1)–P(1)	103.33(3)
Cl(2)–Tc(1)–Cl(1)	135.23(4)	Cl(1)–Tc(1)–P(1)	82.87(4)
Cl(2)–Tc(1)–P(1)	84.56(4)	Cl(2)–Tc(1)–P(2)	82.00(4)
Cl(1)–Tc(1)–P(2)	90.55(4)	P(1)–Tc(1)–P(2)	153.24(4)
Tc(1)–Tc(2)–Cl(4)	112.24(3)	Tc(1)–Tc(2)–Cl(3)	109.72(3)
Tc(1)–Tc(2)–P(3)	102.31(3)	Tc(1)–Tc(2)–P(4)	101.61(3)
Cl(4)–Tc(2)–Cl(3)	138.04(4)	Cl(3)–Tc(2)–P(4)	89.48(4)
Cl(4)–Tc(2)–P(4)	82.29(4)	Cl(4)–Tc(2)–P(3)	87.68(4)
Cl(3)–Tc(2)–P(3)	83.53(4)	P(4)–Tc(2)–P(3)	156.05(4)
C(1)–P(1)–Tc(1)	115.8(2)	C(8)–P(1)–Tc(1)	122.1(2)
C(2)–P(1)–Tc(1)	109.3(2)	C(14)–P(2)–Tc(1)	114.7(2)
C(21)–P(2)–Tc(1)	105.0(2)	C(15)–P(2)–Tc(1)	125.7(2)
C(27)–P(3)–Tc(2)	115.1(2)	C(28)–P(3)–Tc(2)	111.6(2)
C(34)–P(3)–Tc(2)	120.8(2)	C(40)–P(4)–Tc(2)	115.2(2)
C(47)–P(4)–Tc(2)	109.9(2)	C(41)–P(4)–Tc(2)	122.2(1)

5.7%. All non-hydrogen atoms were refined with anisotropic thermal parameters. Hydrogen atoms were placed at calculated positions and included in the structure factor calculation, but their positions were not refined. Final least-squares refinement of 201 parameters resulted in residuals, R (based on F) and R_w (based on F^2),[19] of 0.025 and 0.066, respectively. The largest remaining peak in the final Fourier difference map was 0.64 e/Å^3, and the quality-of-fit on F^2 was 1.14.

$Tc_2Cl_4(PMePh_2)_4 \cdot C_6H_6$ (4·C_6H_6). Crystals of $Tc_2Cl_4(PMePh_2)_4 \cdot C_6H_6$ were grown by slow evaporation of a solution of **4** dissolved in a mixture of benzene and hexamethyldisiloxane. A crystal having the approximate dimensions of 0.17 × 0.30 × 0.30 mm^3 was selected and coated with a thin layer of epoxy cement. The crystal was then fastened to the end of a glass fiber for intensity measurements. Least-squares refinement of 23 carefully centered reflections in the range $90 < 2\theta < 115°$ resulted in unit cell parameters having primitive monoclinic symmetry. Intensity data were collected at room temperature in the range $4 < 2\theta < 120°$ on a Rigaku AFC5R diffractometer equipped with a rotating Cu source ($\lambda_{Cu\ K\alpha}$ = 1.541 84 Å). A total of 7830 data were collected using a θ–2θ scan motion. A plot of three representative reflections measured at regular intervals revealed no loss in diffraction intensity during the experiment. An absorption correction based on azimuthal scans of several reflections with Eulerian angle χ near 90° was also applied to the data. After averaging of equivalent reflections, there remained 7576 unique data, of which 6549 had $F_o^2 > 2\sigma(F_o^2)$. The positions of the Tc atoms were determined from a Patterson synthesis. The remaining non-hydrogen atoms were located by application of a series alternating least-squares cycles and difference Fourier maps. All non-hydrogen atoms were refined with anisotropic displacement parameters except the carbon atoms of the interstitial benzene molecule. The positions of the carbon atoms of the interstitial benzene molecule were restrained to fit a regular hexagon. Hydrogen atoms were included in the structure factor calculation at idealized positions but were not subsequently refined. Final least-squares refinement of 572 parameters resulted in residuals, R (based on F) and R_w (based on F^2),[19] of 0.035 and 0.100, respectively. After convergence, the quality-of-fit on F^2 was 1.08 and the highest peak in the final difference Fourier map was 0.88 e/Å^3.

Results

Synthesis. A rational, high-yield synthesis has been developed for dinuclear technetium phosphine complexes possessing a metal–metal triple bond. Two-electron reduction of the mononuclear Tc(IV) phosphine complexes $TcCl_4(PR_3)_2$ with finely divided zinc in aromatic solvents or THF results in the formation of Tc(II) compounds $Tc_2Cl_4(PR_3)_4$, where PR_3 = PEt_3, PPr^n_3, $PMePh_2$, and PMe_2Ph (eq 1). The reduction of $TcCl_4(PR_3)_2$ occurs under

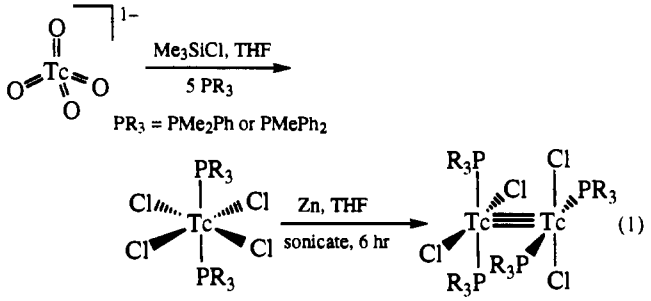

(1)

mild heating (50–55 °C) in toluene or by sonication in benzene or THF using an ultrasonic cleaning bath. Both methods afford **1** in yields of greater than 90%. The sonication reaction is more convenient because of the shorter reaction times and slightly higher yields. Sonication decreases the reaction time by continuously providing a clean surface of zinc for reduction to take place. As the reaction proceeds, the zinc metal is consumed, resulting in the formation of a reddish purple solution. The resulting $ZnCl_2$ byproduct is filtered off, and the dinuclear product may be obtained either by careful addition of heptane or hexamethyldisiloxane or by slow evaporation of a solution containing a mixture of benzene and hexamethyldisiloxane. These new metal–metal bonded complexes are readily soluble in aromatic solvents and CH_2Cl_2, slightly soluble in diethyl ether, and relatively insoluble in acetonitrile, aliphatic hydrocarbons, and hexamethyldisiloxane.

The Tc(IV) precursors used for the preparation of $Tc_2Cl_4(PR_3)_4$ are easily synthesized by phosphine substitution on $TcCl_4(PPh_3)_2$, which is readily prepared from $[NH_4][TcO_4]$ by reduction with excess triphenylphosphine in the presence of HCl (eq 2).[11] For the less basic, aryl-substituted phosphines PMe_2Ph

$$[NH_4][TcO_4] \xrightarrow[HCl]{\text{excess } PPh_3} TcCl_4(PPh_3)_2 \xrightarrow[R = Et,\ Pr^n]{2\ PR_3}$$

$$TcCl_4(PR_3)_2 \xrightarrow[\text{sonicate}]{Zn,\ C_6H_6} Tc_2Cl_4(PR_3)_4 \quad (2)$$

and $PMePh_2$, substitution on $TcCl_4(PPh_3)_2$ is ineffective. Fortunately, these bis-substituted Tc(IV) analogs may be prepared directly from $[NH_4][TcO_4]$ *via* reaction of excess phosphine in the presence of trimethylsilyl chloride instead of HCl(aq) (eq 1). This anhydrous route represents a departure from the previously reported aqueous method used for preparing $TcCl_4(PMe_2Ph)_2$.[20] The yields are comparable to those reported in the literature for the aqueous preparation, but the procedure may be performed in a drybox under inert atmospheric conditions. Furthermore, in order to maximize the yield of the dinuclear complexes, we found it necessary to purify the $TcCl_4(PR_3)_2$ precursors by chromatography prior to reduction in order to remove any $[TcCl_3(PR_3)_3]Cl$ formed in the synthesis of $TcCl_4(PR_3)_2$. We also noted that zinc reduction of $[TcCl_6]^{2-}$ in the presence of phosphine resulted in the formation of mononuclear, phosphine-containing species and not the desired dinuclear complexes, emphasizing the need for phosphine coordination prior to reduction with zinc. Wester and co-workers have successfully used similar sonication techniques to prepare Tc(I) bis(arene) complexes.[21] In the present case, however, complete reduction to Tc(I) species is thwarted by the formation of the $Tc_2Cl_4(PR_3)_4$, which is not susceptible to further reduction as evidenced by cyclic voltammetry studies (*vida infra*).

Spectroscopic Properties. The compounds $Tc_2Cl_4(PR_3)_4$ (PR_3 = PEt_3, PPr^n_3, PMe_2Ph, $PMePh_2$) are diamagnetic as evidenced by their relatively sharp and unshifted ^1H and ^{31}P NMR spectra (Table 8). The absence of paramagnetism is consistent with the formation of a metal–metal bond between two Tc(II) centers; a mononuclear Tc(II) would be expected to have one unpaired electron. The $^{31}P\{^1H\}$ NMR spectrum of each species reveals a single resonance shifted well downfield from that of the free phosphine and indicates that the phosphines are chemically equivalent. The ^1H NMR resonances for **3** and **4** are quite similar in that they exhibit a set of multiplets at δ 7.0 and 7.6 for the phenyl protons and a virtual triplet for the methyl groups at δ 1.6, consistent with the presence of mutually *trans* phosphine ligands. The ^1H NMR spectra for the trialkylphosphine complexes **1** and **2** show a series of multiplets for the aliphatic protons as a result of proton–phosphorus coupling superimposed on the expected proton–proton coupling for these groups.

The electronic spectra for compounds **1**–**4** show a series of very weak absorptions between 488 and 770 nm. (Table 8). Comparison of the electronic spectra of $Tc_2Cl_4(PR_3)_4$ with those of $Re_2Cl_4(PR_3)_4$ suggests that the two series of compounds have identical ground state electron configurations.[22] The low molar absorptivities for these transitions are consistent with spin and orbitally forbidden transitions found for other M–M bonded complexes containing an electron-rich $\sigma^2\pi^4\delta^2\delta^{*2}$ triple bond. It is likely that the low-energy band near 770 nm corresponds to a forbidden $\delta^* \rightarrow \sigma^*$ excitation by analogy with the visible spectrum of $Re_2Cl_4(PPr^n_3)_4$.[23]

(20) Mazzi, U.; De Paoli, G.; Di Bernardo, P.; Magon, L. *J. Inorg. Nucl. Chem.* **1976**, *38*, 721.
(21) Wester, D. W.; Coveney, J. R.; Nosco, D. L.; Robbins, M. S.; Dean, R. T. *J. Med. Chem.* **1991**, *34*, 3284.
(22) Ebner, J. R.; Walton, R. A. *Inorg. Chem.* **1975**, *14*, 1987.
(23) Bursten, B. E.; Cotton, F. A.; Fanwick, P. E.; Stanley, G. G.; Walton, R. A. *J. Am. Chem. Soc.* **1983**, *105*, 2606.

Table 8. Spectroscopic Data for $Tc_2Cl_4(PR_3)_4$ Complexes

	^1H NMR[a] δ, ppm	$^{31}P\{^1H\}$[b] δ, ppm	electronic data[c] λ_{max}, nm (ϵ, M^{-1} cm^{-1})
$Tc_2Cl_4(PEt_3)_4$	2.25 (m), 1.02 (m)	+47.5 (s)	770 (30), 648 (30), 528 (sh), 496 (56)
$Tc_2Cl_4(PPr^n_3)_4$	2.33 (m), 1.51 (m), 0.99 (m)	+44.3 (s)	748 (15), 588 (22), 534 (sh), 488 (54)
$Tc_2Cl_4(PMe_2Ph)_4$	7.62 (m), 6.99 (m), 1.60 (t)	+42.6 (s)	752 (25), 622 (30), 528 (64), 488 (75)
$Tc_2Cl_4(PMePh_2)_4$	7.63 (m), 6.99 (m), 1.60 (t)	+39.5 (s)	770 (33), 660 (47), 566 (sh), 510 (114)

[a] Measured in C_6D_6 at 300 MHz. [b] Measured in C_6D_6 at 121.5 MHz. [c] Measured in C_6H_6.

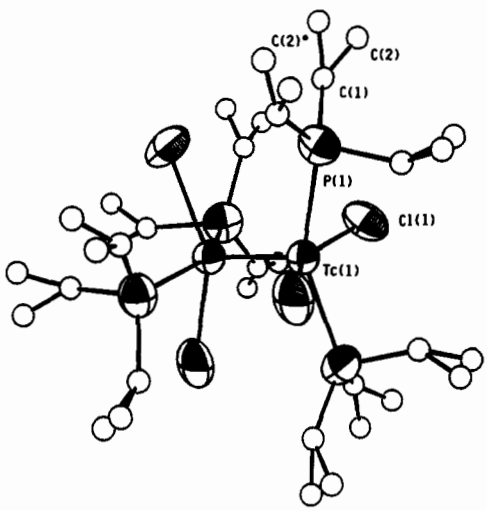

Figure 1. ORTEP drawing of $Tc_2Cl_4(PEt_3)_4$ (**1**) showing one orientation of the metal–metal bond. The ethyl carbons are shown as spheres of arbitrary size for clarity. The β-carbon atoms of the ethyl groups are disorder equally over two sites.

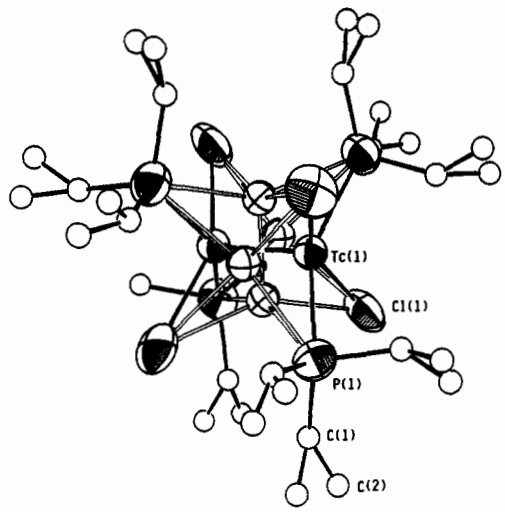

Figure 2. ORTEP drawing of $Tc_2Cl_4(PEt_3)_4$ (**1**) showing the three-way disorder of the Tc–Tc bond.

Molecular Structures. The solid-state molecular structures have been determined for $Tc_2Cl_4(PR_3)_4$, PR_3 = PEt_3 (**1**), PMe_2Ph (**3**), and $PMePh_2$ (**4**).[24] Crystallographic parameters and basic information pertaining to data collection and structure refinement are summarized in Table 1. Selected bond distances and angles are listed in Tables 5–7 for compounds **1**, **3**, and **4**·C_6H_6.

$Tc_2Cl_4(PEt_3)_4$ (1). The alkylphosphine derivative $Tc_2Cl_4(PEt_3)_4$ crystallizes in a body-centered cubic lattice and is isomorphous with the analogous rhenium compound $Re_2Cl_4(PEt_3)_4$.[17] The metal–metal bond resides on a crystallographic site with $\bar{4}3m$ symmetry. As a result, the Tc–Tc unit is equally disordered over three mutually perpendicular sites. Furthermore, the chloride and phosphine ligands lie on $3m$ positions. This requires the ethyl substituents of the phosphine to lie on the mirror plane. However, as illustrated (Figure 1) in the ORTEP diagram of **1**, the β-carbon of the ethyl group is slightly shifted off this plane, creating a disorder over two sites. This disorder leads to the highly distorted bond distances observed for the ethyl groups. The shape of the molecule allows it to pack on the same lattice sites but oriented in three orthogonal directions. This creates the observed disordering of the Tc–Tc bond (Figure 2). The packing, however, is not ideal, and the three orientations have slightly different atomic positions for the ligands that are crystallographically indistinguishable. As a result, the observed Tc–P and Tc–Cl bond distances and associated angles are not in fact correct for any one of the different orientations. Similar discrepancies were noted in the other similarly disordered structures of $Mo_2Cl_4(PEt_3)_4$ and $Re_2Cl_4(PEt_3)_4$.[17] The high crystallographic symmetry further requires the dinuclear unit to adopt a rigorously eclipsed conformation of the *trans*-$TcCl_2L_2$ halves of the molecule. The Tc–Tc bond distance of 2.133(3) Å is shorter than the Re–Re distance observed for $Re_2Cl_4(PEt_3)_4$ (2.250(4) Å) but comparable to the Mo–Mo distance in $Mo_2Cl_4(PEt_3)_4$ (2.132(5) Å).[17]

$Tc_2Cl_4(PMe_2Ph)_4$ (3). An ORTEP diagram of $Tc_2Cl_4(PMe_2Ph)_4$ is presented in Figure 3. The molecule crystallizes with the

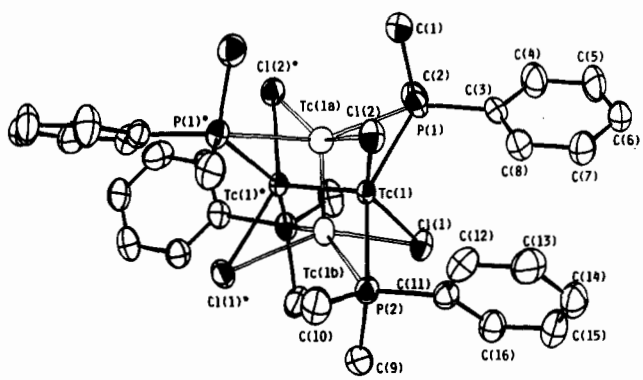

Figure 3. ORTEP drawing of $Tc_2Cl_4(PMe_2Ph)_4$ (**3**) depicting the primary (Tc(1) and Tc(1)*) and secondary (Tc(1a) and Tc(1b)) orientations of the metal–metal bond. Probability ellipsoids are at the 40% level.

Tc–Tc vector perpendicular to a crystallographic C_2 axis. The structure is made up of two *trans*-$TcCl_2(PMe_2Ph)_2$ fragments that are rotated 90° with respect to each other to give an eclipsed geometry with approximate D_{2d} symmetry. The P(1)–Tc(1)–Tc(1)*–Cl(2)* torsion angle is 6.58(5)°. The Tc–Tc bond distance is 2.127(1) Å and is the shortest of the three reported here. It is similar to the M–M distance observed for $Mo_2Cl_4(PMe_2Ph)_4$[25] but shorter than that in the analogous Re complex $Re_2Cl_4(PMe_2Ph)_4$.[26] The *trans*-$TcCl_2(PMe_2Ph)_2$ fragments are quite distorted from planarity as a result of steric repulsion between the ligands. This distortion is reflected in the P(1)–Tc(1)–P(2) and Cl(1)–Tc(1)–Cl(2) bond angles of 150.24(5) and 143.51(5)°, respectively. The average Tc–P and Tc–Cl bond distances, 2.45[1] and 2.394[2] Å, are slightly longer than analogous distances in the Re complex (2.418[2] and 2.387[3] Å).[26] The shorter M–M bond distance for $Tc_2Cl_4(PMe_2Ph)_4$ relative to $Re_2Cl_4(PMe_2Ph)_4$ forces the Tc–P and Tc–Cl bond distances to be slightly longer than the corresponding metal–ligand distances in $Re_2Cl_4(PMe_2Ph)_4$, even though the atomic radius of Tc is slightly smaller than that of Re. The phosphine ligands are oriented so

(24) Unit cell parameters were also determined for $Tc_2Cl_4(PPr^n_3)_4$: $C222_1$ with a = 14.915(4) Å, b = 17.464(5) Å, c = 24.263(7) Å, V = 6320(3) Å^3, and Z = 8.

(25) Cotton, F. A.; Daniels, L. M.; Powell, G. L.; Kahaian, A. J.; Smith, T. J.; Vogel, E. F. *Inorg. Chim. Acta* **1988**, *144*, 109.

(26) Cotton, F. A.; Dunbar, K. R.; Falvello, F. R.; Tomas, M.; Walton, R. A. *J. Am. Chem. Soc.* **1983**, *105*, 4950.

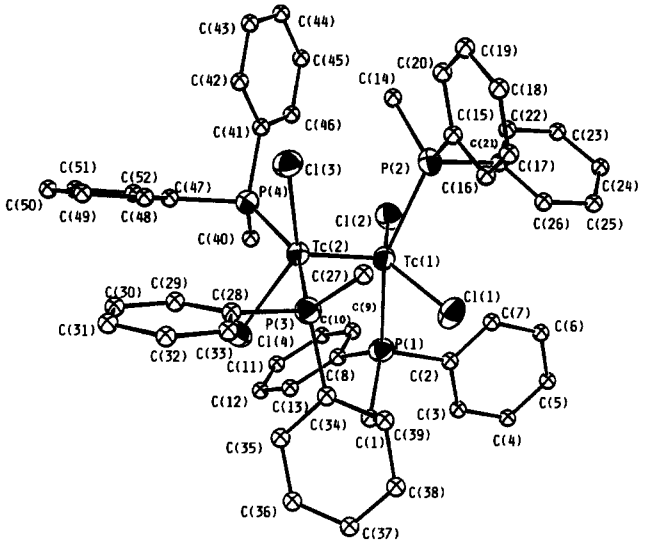

Figure 4. ORTEP drawing of $Tc_2Cl_4(PMePh_2)_4$ (**4**) with 40% probability ellipsoids. For clarity, carbons atoms are shown as spheres of arbitrary size.

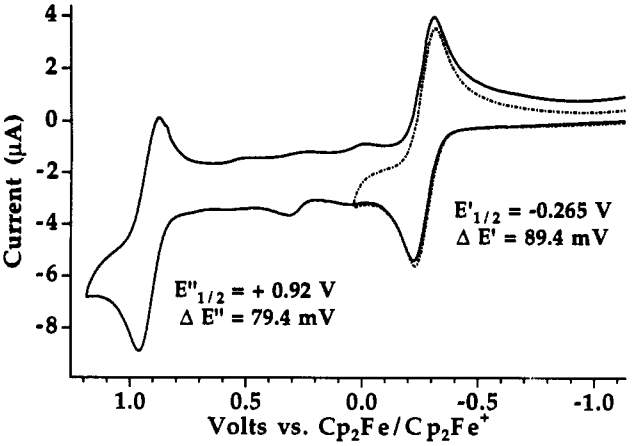

Figure 5. Cyclic voltammogram of $Tc_2Cl_4(PMe_2Ph)_4$ (**3**) in CH_2Cl_2 at a scan rate of 200 mV s^{-1}.

Table 9. Electrochemical Data for $M_2Cl_4(PR_3)_4$ Complexes of Tc and Re

	$E_{1/2,ox}(1)^a$	$E_{1/2,ox}(2)^a$	ref
$Tc_2Cl_4(PEt_3)_4^b$	–0.48	0.88	this work
$Tc_2Cl_4(PPr^n_3)_4^b$	–0.49	0.89	this work
$Tc_2Cl_4(PMe_2Ph)_4^b$	–0.26	0.92	this work
$Tc_2Cl_4(PMePh_2)_4^b$	–0.26	0.92	this work
$Re_2Cl_4(PEt_3)_4^c$	–0.73	0.49	29
$Re_2Cl_4(PPr^n_3)^c$	–0.75	0.48	29
$Re_2Cl_4(PMe_2Ph)_4^c$	–0.61	0.51	29

[a] Volts vs Cp_2Fe/Cp_2Fe^+. [b] Measured in CH_2Cl_2 with 0.2 M $[^nBu_4N][BF_4]$ as a supporting electrolyte at a scan rate of 200 mV s^{-1} using a Pt disk electrode. [c] Originally referenced vs SCE but converted to volts vs Cp_2Fe/Cp_2Fe^+, assuming 0.0 V SCE ≈ –0.31 V vs Cp_2Fe/Cp_2Fe^+.

that the phenyl rings are approximately parallel with the Tc–Tc bond and are directed away from the metal–metal bond.

In addition to the major orientation of the metal–metal bond, a second, minor, orientation exists in which the Tc–Tc bond is collinear with the crystallographic C_2 axis that bisects the Tc–Tc bond of the major orientation. The occupancy for the second orientation is 5.7(1)%. A similar disorder was also observed in the dirhenium compound $Re_2Cl_4(PMe_2Ph)_4$ but was not seen in the structure of $Mo_2Cl_4(PMe_2Ph)_4$. The minor orientation is not simply a disorder of the $M_2Cl_4(PR_3)_4$ units, but rather it corresponds to a different conformational isomer. In the primary conformation the chlorine atoms reside in clefts that are bracketed by the phenyl ring and a methyl group of the *cis*-phosphine ligands (Figure 3). In the minor conformation, the Cl atoms are bracketed by the phenyl ring and a methyl group on one side and by two methyl groups on the other side. Furthermore, the phenyl rings of the phosphines are projected perpendicular to the Tc–Tc bond instead of parallel to it. The preference for one conformation over the other probably originates in the interaction of the Cl atoms with clefts formed by the substitutents on the phosphine ligands that are *cis* to the chloride atoms. The interaction with clefts that are made up of two sp^3-hybridized carbons are apparently less favorable than those bracketed by an sp^3- and an sp^2-hybridized carbon.

$Tc_2Cl_4(PMePh_2)_4 \cdot C_6H_6$ ($4 \cdot C_6H_6$). Slow evaporation of a solution of $Tc_2Cl_4(PMePh_2)_4$ in a mixture benzene and hexamethyldisiloxane resulted in the crystallization of **4** with an interstitial molecule of benzene. This crystalline form is isomorphous with the analogous C_6H_6 solvate of $Mo_2Cl_4(PMePh_2)_4$.[27] The dinuclear unit resides on a general position and overall has D_{2d} symmetry despite the lack of any crystallographically imposed symmetry. An ORTEP diagram presented in Figure 4 shows the molecular geometry of the dinuclear complex. Similar to those of the other $Tc_2Cl_4(PR_3)_4$ complexes, the two *trans*-$TcCl_2(PR_3)_2$ fragments are essentially eclipsed, as evidenced by the P(1)–Tc(1)–Tc(2)–Cl(4) torsion angle of 3.54(4)°. The Tc–Tc bond distance of 2.1384(5) Å is comparable to those observed for the other $Tc_2Cl_4(PR_3)_4$ species. Just as in the structure of $Tc_2Cl_4(PMe_2Ph)_4$, the Tc–P and Tc–Cl bond distances are slightly longer than analogous distances observed in the dirhenium compound despite the smaller atomic radius of Tc.

Only one orientation of the Tc–Tc bond was found for $Tc_2Cl_4(PMePh_2)_4 \cdot C_6H_6$. The phosphine ligands are so arranged that the chlorine atoms reside in clefts described by the two phenyl rings of one *cis*-phosphine and by a phenyl ring and one of the methyl groups of the other *cis*-phosphine. The incorporation of a second orientation perpendicular to the Tc–Tc bond would create a conformational isomer in which the Cl atoms were bracketed only by mixed pairs of methyl and phenyl groups on both sides. This is clearly an unfavorable arrangement. The phosphines are rotated about the Tc–P bond and give rise to a pseudo-S_4 symmetry axis collinear with the metal–metal bond. Similar ligand conformations with pseudo-S_4 symmetry were observed for $Mo_2Cl_4(PMePh_2)_4$ and $Re_2Cl_4(PMePh_2)_4$, both of which exhibited only one orientation of the metal–metal bond.[27]

Electrochemistry. Electrochemical studies were performed on $Tc_2Cl_4(PR_3)_4$ (PR_3 = PEt_3, PPr^n_3, PMe_2Ph, $PMePh_2$) in methylene chloride using a 0.2 M solution of $[^nBu_4N][BF_4]$ as a supporting electrolyte. The cyclic voltammograms for compounds **1**–**4** show two reversible one-electron oxidation couples. The cyclic voltammogram of $Tc_2Cl_4(PMe_2Ph)_4$ shown in Figure 5 is representative of the electrochemical behavior exhibited by each compound. The electrochemical half-wave potentials for these dinuclear species are listed in Table 9 and are referenced to an internal ferrocene standard. For comparison, the $E_{1/2}$ values for several $Re_2Cl_4(PR_3)_4$ species are also listed in Table 9.[28] The oxidation couples remained reversible at the scan speeds ranging from 200 down to 20 mV s^{-1}. The oxidation potentials indicate that the aryl-substituted phosphine complexes **3** and **4** are slightly more difficult to oxidize than the trialkylphosphine complexes **1** and **2**, presumably because of the better electron-donating properties of the alkylphosphines. Similar redox behavior was observed for the analogous $Re_2Cl_4(PR_3)_4$ complexes.[29] The oxidation half-waves of the ditechnetium compounds appear at more positive potentials than those of the corresponding dirhenium complexes. This is in keeping with the general trend that third-

(27) Cotton, F. A.; Czuchajowska, J.; Luck, R. L. *J. Chem. Soc., Dalton Trans.* **1991**, 579.

(28) All values have been referenced to the Cp_2Fe/Cp_2Fe^+ couple.

(29) Brant, P.; Salmon, D. J.; Walton, R. A. *J. Am. Chem. Soc.* **1978**, *100*, 4424.

row transition metal complexes, whether they are mono- or dinuclear, are oxidized more readily than their second-row congeners.

By analogy with $Re_2Cl_4(PR_3)_4$, these oxidation processes correspond to the removal of first one and then the second electron from the filled δ^* orbital to yield ditechnetium species with $\sigma^2\pi^4\delta^2\delta^*$ and $\sigma^2\pi^4\delta^2$ electronic configurations. The reversible nature of the oxidation couples indicates that (at least on the electrochemical time scale) removal of δ^* electrons engenders no major structural changes. As a result, chemical oxidation should allow for the synthesis of cationic complexes of the type $[Tc_2Cl_4(PR_3)_4]^+$ and $[Tc_2Cl_4(PR_3)_4]^{2+}$. Attempts to isolate and characterize these new Tc_2^{5+} and Tc_2^{6+} species are in progress; the results of these efforts will be reported in due course.

Discussion

The synthetic procedures presented here describe a rational, stepwise route to several new dinuclear species of the type $Tc_2Cl_4(PR_3)_4$ where $PR_3 = PEt_3$, PPr^n_3, PMe_2Ph, and $PMePh_2$. These compounds are the first examples of phosphine complexes that contain a Tc–Tc multiple bond. The synthetic procedure takes advantage of the ready availability of midvalent technetium phosphine compounds as precursors to lower valent dinuclear species. The principal advantage in using $TcCl_4(PR_3)_2$, however, lies in the fact that the requisite number of phosphine ligands are already present. Traditional methods used to synthesize $M_2Cl_4(PR_3)_4$ type complexes involve the reduction of a metal precursor in the presence of excess phosphine ligand. For example, the analogous rhenium compounds, $Re_2Cl_4(PR_3)_4$, are prepared by heating $[Re_2Cl_8]^{2-}$ with an excess of the appropriate phosphine.[22a] In this reaction, the phosphine not only displaces the chloride ligands but also acts as a reducing agent. However, under such conditions, there is also the possibility of forming mononuclear phosphine complexes by cleavage of the metal–metal bond. While this is not a problem in the rhenium chemistry, preliminary studies indicate that $[Tc_2Cl_8]^{2-}$ undergoes metal–metal bond scission in the presence of excess phosphine to yield mononuclear Tc species.[30] To avoid such reactions, it is vital to limit the amount of phosphine that is present. One means of accomplishing this is by using a precursor, in this case $TcCl_4(PR_3)_2$, that already has the required number of phosphine ligands. Two-electron reduction of $TcCl_4(PR_3)_2$ accompanied by loss of two chloride ions yields two $TcCl_2(PR_3)_2$ fragments that, in the absence of a suitable ligand, combine to form the desired dinuclear complex, $Tc_2Cl_4(PR_3)_4$. It is possible that such an approach could be exploited to prepare other dinuclear complexes that are currently unknown, *e.g.* $[Ru_2Cl_4(PR_3)_4]^{n+}$ and $[Os_2Cl_4(PR_3)_4]^{n+}$.

The spectroscopic properties of $Tc_2Cl_4(PR_3)_4$ ($PR_3 = PEt_3$, PPr^n_3, PMe_2Ph, $PMePh_2$) are those expected for an electron-rich, metal–metal triple bond. The similarity of the electronic absorption spectra of the $Tc_2Cl_4(PR_3)_4$ compounds to the electronic spectra of their rhenium analogs is consistent with a ground-state $\sigma^2\pi^4\delta^2\delta^{*2}$ electron configuration. Further support is provided by the observation of two reversible oxidations. These oxidations correspond to sequential removal of electrons from the filled δ^* orbital to give the oxidized dimers with Tc_2^{5+} and Tc_2^{6+} cores.

X-ray crystallographic studies performed on the PEt_3, PMe_2Ph, and $PMePh_2$ derivatives reveal that each complex adopts an eclipsed M_2L_8 conformation typical of other $M_2Cl_4(PR_3)_4$ (M = Mo, W, Re) species. Since the $\sigma^2\pi^4\delta^2\delta^{*2}$ electron configuration dictates no angular requirements on the orientation of the two *trans*-$TcCl_2(PR_3)_2$ fragments, it is clear that the steric requirements of the phosphines force these units to be eclipsed. The Tc–Tc distances are virtually invariant and show no correlation with phosphine basicity. A similar lack of correlation of metal–metal bond distance and phosphine basicity was also noted for a series of $Mo_2Cl_4(PR_3)_4$ complexes.[25]

The only other example of a Tc–Tc triple bond is that found in the extended-chain structure of $[Tc_2Cl_6]_n^{2n-}$ in which two chloride ligands on each metal are shared with a neighboring dinuclear fragment.[9] The Tc–Tc bond distance in this material is 2.044(1) Å and is considerably shorter than those found for $Tc_2Cl_4(PR_3)_4$. In fact, this distance is the shortest observed for an unbridged metal–metal bonded complex of technetium.[31] One explanation that has been put forth for this short distance is that reduction of the effective nuclear charge on the metal centers enhances the σ and π bonding sufficiently to offset the occupation of the δ^* orbital, resulting in a substantial contraction in the Tc–Tc bond distance. However, the bond distances found for the $Tc_2Cl_4(PR_3)_4$ complexes presented here are considerably longer. Most likely, this can be attributed to the steric requirements of the bulky phosphine ligands. In order to draw conclusions about the influence of the δ^* bond on the Tc–Tc separation, a series of complexes must be compared in which the ligand set remains unchanged. The fact that $[Tc_2Cl_6]_n^{2n-}$ contains some chloride ligands that are shared between dinuclear units spoils the comparison with $[Tc_2Cl_8]^{2-}$ and $[Tc_2Cl_8]^{3-}$, which both exist as discrete entities in the solid state. The existence of two reversible one-electron oxidations for $Tc_2Cl_4(PR_3)_4$ suggests that it may be possible to chemically oxidize the compounds in successive one-electron steps to yield the corresponding Tc_2^{5+} and Tc_2^{6+} complexes without causing major structural reorganization. A structural study of such a series would yield valuable information regarding the concomitant effects of changes in charge and the δ^* bond on Tc–Tc bond distances.[32] We intend to pursue these investigations.

Acknowledgment. This work was supported by the Laboratory Directed Research and Development Program at Los Alamos National Laboratory. The authors also acknowledge financial assistance from the National Science Foundation and the Laboratory for Molecular Structure and Bonding for support of the facilities at Texas A&M University. We thank Dr. Lee Daniels (Texas A&M) for crystallographic assistance, Dr. Jeffrey Bryan (LANL) for helpful discussions, and Dr. Robert Hightower (Oak Ridge National Laboratory) for a generous gift of ammonium pertechnetate.

Supplementary Material Available: Tables of crystallographic parameters, hydrogen positional and isotropic thermal parameters, complete bond distances and angles, and anisotropic thermal parameters for the non-hydrogen atoms (29 pages). Ordering information is given on any current masthead page.

(30) Cotton, F. A.; Haefner, S. C.; Sattelberger, A. P. Unpublished observations.

(31) A shorter Tc–Tc distance has been claimed for the compound $[(C_5Me_5)Tc(\mu\text{-}O)_3Tc]_n$ [Kanellakopulos, B.; Nuber, B.; Raptis, K.; Ziegler, M. L. *Angew. Chem., Int. Ed. Engl.* **1989**, *28*, 1055], but the entire structure and identity of this substance are in question.

(32) A similar study has been performed on the series of compounds $[Re_2Cl_4(PMe_2Ph)_4]^{n+}$ where n = 0–2. See ref 26.